- Supporting Information -

Oxygen Reduction Reaction Causes Iron Leaching from Fe-N-C Electrocatalysts

Yu-Ping Ku[a,b,*], Konrad Ehelebe[a,b], Markus Bierling[a,b], Florian D. Speck[a,b], Dominik Seeberger[a,b], Karl J.J. Mayrhofer[a,b], Simon Thiele[a,b], Serhiy Cherevko[a,*]

[a] Forschungszentrum Jülich GmbH, Helmholtz-Institute Erlangen-Nürnberg for Renewable Energy (IEK-11), Cauerstraße 1, 91058 Erlangen, Germany

[b] Department of Chemical and Biological Engineering, Friedrich-Alexander University Erlangen-Nürnberg, Cauerstraße 1, 91058 Erlangen, Germany

[*] corresponding authors: y.ku@fz-juelich.de, s.cherevko@fz-juelich.de

Table of contents

1. Supporting results

1.1 Online dissolution results

The online dissolution results were obtained with a gas diffusion electrode setup coupled to inductively coupled plasma mass spectrometry (GDE-ICP-MS), which has been introduced in our previous work.[1]

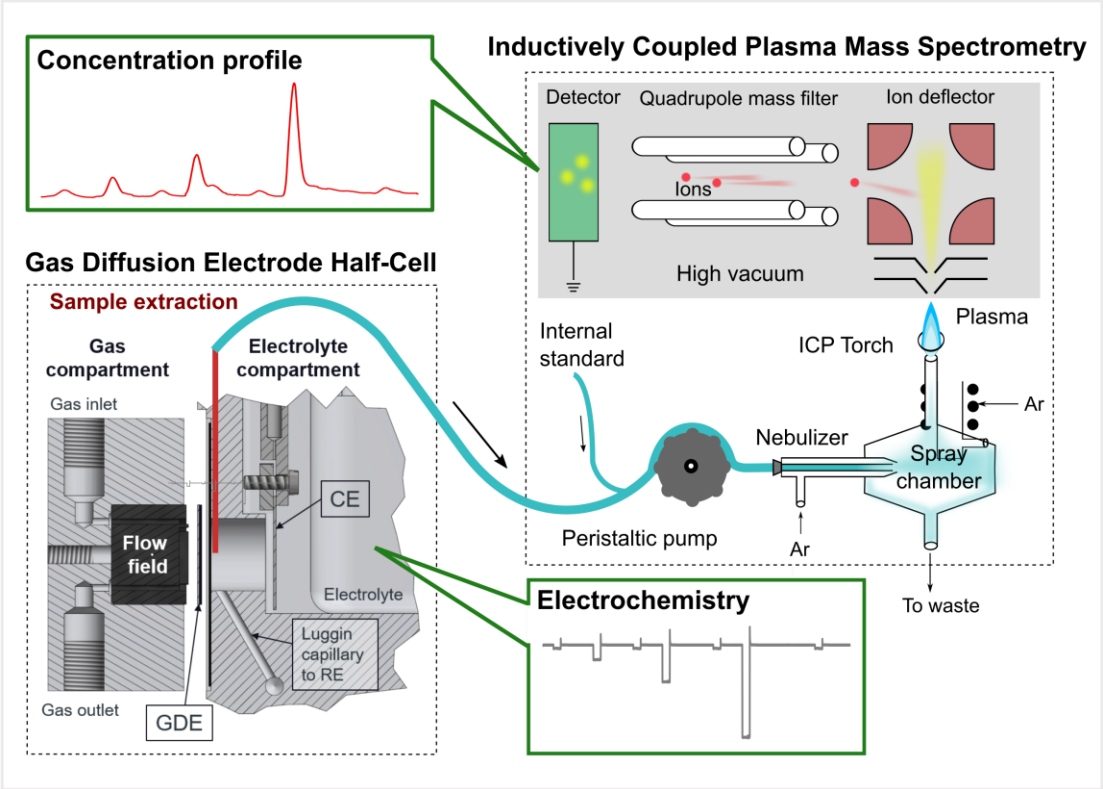

Scheme S1. Scheme of the gas diffusion electrode half-cell setup coupled to inductively coupled plasma mass spectrometry (GDE-ICP-MS)[1] used in this work to detect online dissolution in realistic catalyst layers.

Figure S1 shows the ignorable impact of the step order during the chosen protocol before the accelerated stress test (AST) on the potential response (activity, Figure S1B) of and Fe dissolution (stability, Figure S1C) from the Fe-N-C gas diffusion electrodes (GDEs).

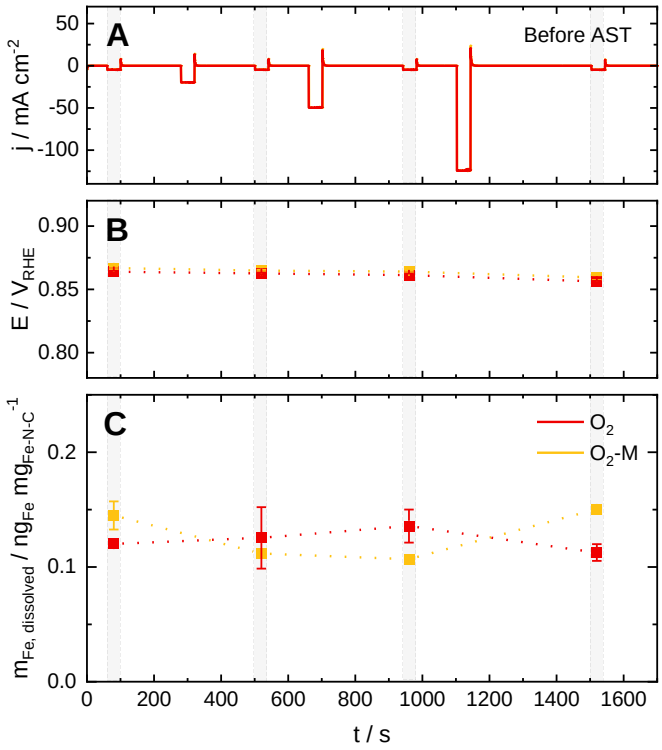

Figure S1. A: Electrochemical (Galvanostatic) protocol before the AST in the presence of O_2. B & C: The electrochemical potential (B) of and the amount of dissolved Fe species (C) from the Fe-N-C GDEs without and with the anion exchange membrane (AEM, HNN5-00-X, Ionomr), O_2 and O_2-M, respectively, during the regularly repeated galvanostatic holds at -5 mA·cm^{-2}.

Figure S2 suggests the Fe dissolution during oxygen reduction reaction (ORR) is highly dependent on the applied charge instead of the number of the potential cycles.

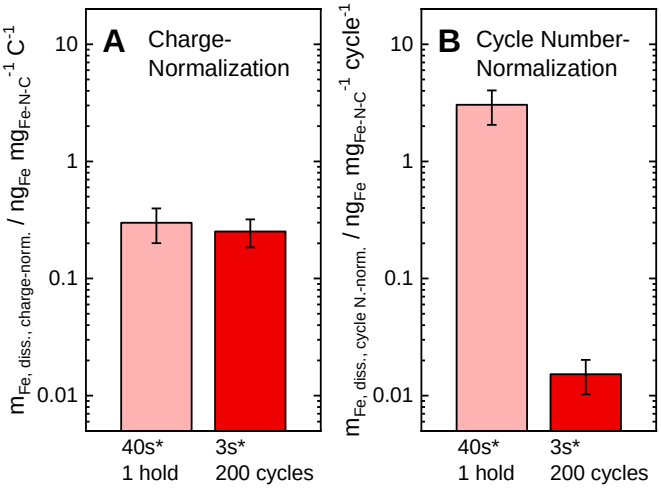

Figure S2. Comparison of (A) charge- and (B) cycle-number-normalization methods applied on the integrated Fe dissolution during two different electrochemical techniques, a 40-s galvanostatic hold at -125 $mA \cdot cm^{-2}$ and the AST (200 times of 3-s galvanostatic holds at -125 $mA \cdot cm^{-2}$), in an O_2-saturated alkaline (0.1 M NaOH) media.

Figure S3 displays the trivial impacts of the doctor-blade coated anion exchange membrane (AEM) on the potential response (activity, Figure S3B) of and Fe dissolution (stability, Figure S3C) from the Fe-N-C GDEs during ORR.

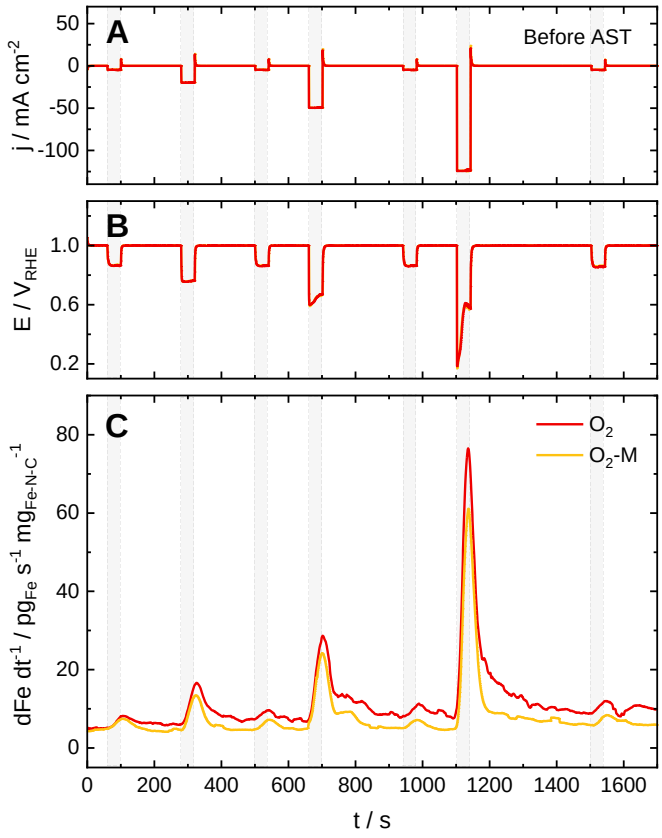

Figure S3. Comparison of Fe demetallation in the Fe-N-C GDEs without (O_2, red) and with (O_2-M, yellow) a doctor-blade coated AEM (HNN5-00-X, Ionomr) in a O_2-saturated alkaline (0.1 M NaOH) environment before the AST. A: Current density profile. B: Potential profile. C: Fe dissolution profile normalized to catalyst loading.

1.2 Structural analysis

Figure S1 Figure S4A is a cross-sectional scanning electron microscope (SEM) image of the Fe-N-C GDE without AEM and Figure **S4**B is a cross-sectional focused ion beam (FIB)-SEM image of the thin AEM on a Fe-N-C catalyst layer (CL). From these images, the thicknesses of the Fe-N-C CL and the AEM, and thus their ratio can be obtained. In Table **S1**, these are summarized and compared to those from the previous work of Ehelebe et al.[1]

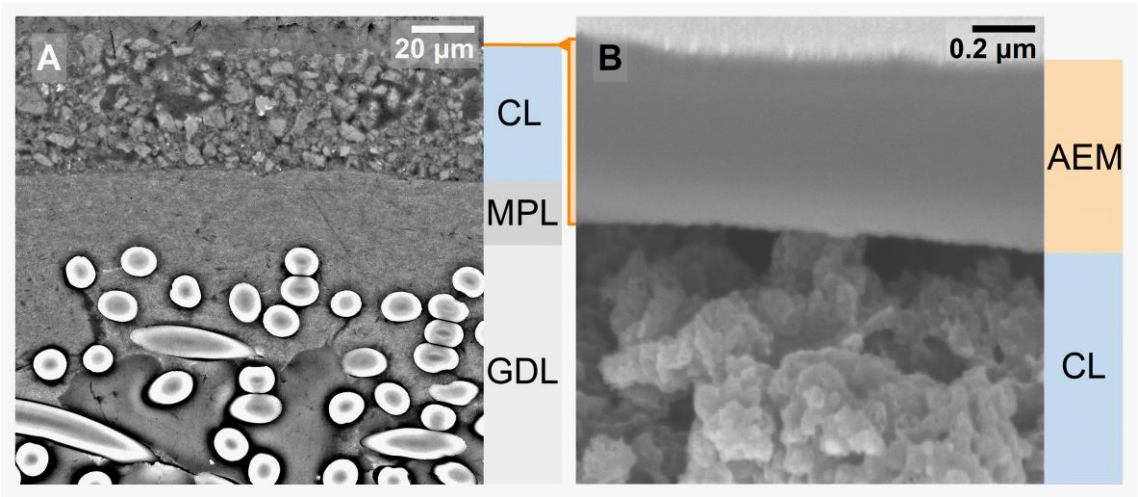

Figure S4. A: Cross-sectional scanning electron microscope (SEM) image of the Fe-N-C GDE without AEM. The GDE includes a gas diffusion layer (GDL), a microporous layer (MPL), and a catalyst layer (CL). B: Cross-sectional focused ion beam scanning electron microscope (FIB-SEM) image of the thin AEM on a Fe-N-C CL. Note that the scale bars of the two images differ by a factor of 100 and that the position of the AEM is indicated with the orange arrow.

Table S1. Comparison of the thicknesses of the CLs and membranes in this work and the previous work of Ehelebe et al.[1]

Catalyst / Media	Thickness of CL (µm)	Thickness of Membrane (µm)	thickness ratio of CL to membrane	Reference
Fe-N-C / Alkaline	47.5 ± 5.2 (Figure S4A)	0.5 ± 0.2 (Figure S4B)	95 : 1	This work
Pt/C / Acidic	4 ± 3	25.4	0.16 : 1	Ehelebe 2021[1]
		50.8	0.08 : 1	

1.3 Electrochemical results

The cyclic voltammograms in Figure S5 present the Fe^{3+}/Fe^{2+} redox transition peaks in the negative-going potential scan of the pristine samples without and with the thin AEM. The onsets and the maximums of the peaks are at around 0.66 and 0.385 $\pm$ 0.015 V_{RHE}, respectively. This suggests at least part of the Fe species would undergo the redox transition in the potential cycling range between 0.57 and 1.0 V_{RHE} in Ar environment.

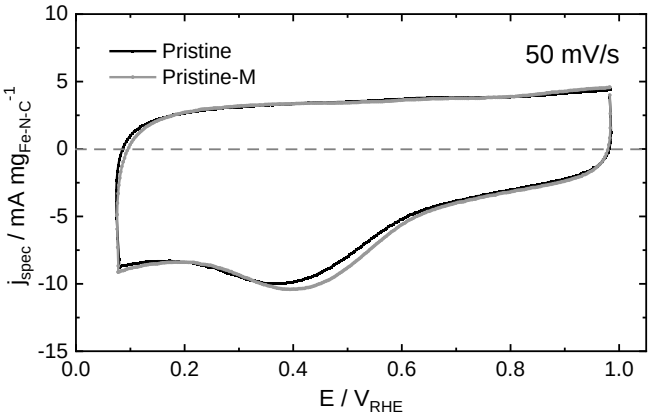

Figure S5. Cyclic voltammograms of the pristine Fe-N-C GDEs without and with a doctor-blade coated AEM (HNN5-00-X, Ionomr) in 0.1 M NaOH (Ar purge: 50 ml·min^{-1}).

2. Supporting discussion

Based on the finding that the Fe dissolution is found to be proportional to the applied charge instead of the number of potential cycles (see Figure S2), the applied AST would correspond to the beginning stage of a FC testing, particularly the first 10 minutes. Nevertheless, it is still not a trivial test or scope because after this AST in an O_2 environment, we observe more than 10% performance drop (see Figure 3B). Moreover, Figure S6 shows that unlike the Fe dissolution before the AST (grey), that after the AST (red) decreases with time. Therefore, the obtained S-number can represent the stability of the studied Fe-N-C catalyst in the corresponded time scope discussed above, yet it would become less representative at a later stage of FC operation. Thus, if this S-number is used to extrapolate the time when half of the Fe active sites are dissolved, the result would be much shorter than what would be observed in AEMFCs. Consequently, future work of longer durability test in a GDE-ICP-MS setup would be needed to obtain the S-number as a function of operation time.

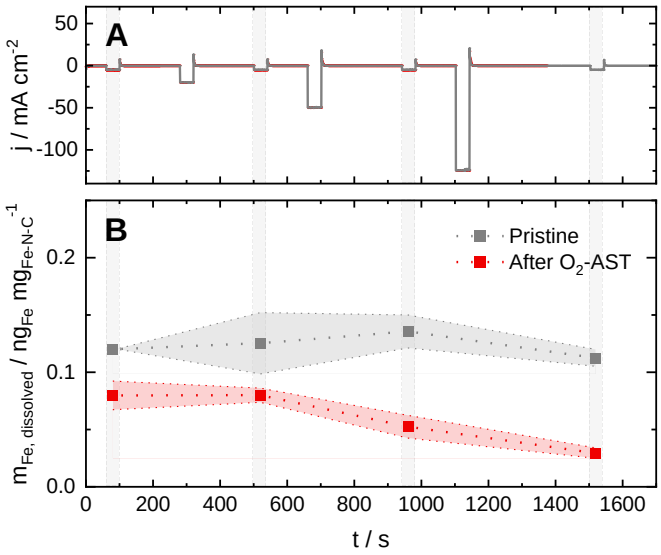

Figure S6. A: Electrochemical (Galvanostatic) protocol before and after the AST in the presence of O_2, noted as pristine and after O_2-AST, respectively. B: The amount of dissolved Fe species from the Fe-N-C GDEs without the AEM during the regularly repeated galvanostatic holds at -5 mA·cm^{-2}.

3. Experimental details

3.1 Electrode manufacturing

The alkaline Fe-N-C gas diffusion electrodes (GDEs) were fabricated by doctor-blade coating an ink onto a gas diffusion media including a microporous layer (H23C8, Freudenberg, 4x4 cm^2, 218 ± 5 μm). The ink was composed of 18 ± 0.3 wt% solids in 1-propanol, and the solid fraction comprised of 70 ± 0.3 wt% a commercial Fe-N-C catalyst (PMF-011904, Pajarito Powder) and 30 ∓ 0.3 wt% a commercial ionomer (Aemion^{TM} HNN5-00-X, Ionomr). Firstly, the ionomer was fully dissolved in the solvent, and then the catalyst powder was added to the solution. The resulting ink was stirred for 30 min, ultra-sonicated for one hour, and then stirred until usage. Subsequently, the ink was applied onto the gas diffusion media with an automated film applicator (ZAA 2300, Zehntner) as the plate temperature was set to 30 ℃. By individually adapting the gap height on the doctor blade the ink film thickness was set to 200 μm. Next, the samples were dried at 60 ℃ for one hour under atmospheric pressure and then one more hour under reduced pressure. By measuring the weights of the GDE samples before the ink deposition and after the drying procedure, the loading of the CLs can be determined to be 1.35 ± 0.05 $mg \cdot cm^{-2}$. As for the anion exchange membrane (AEM) fabrication, a solution comprised of 8 wt% the ionomer in a solvent mixture of 50 wt% 1-propanol in water was doctor-blade coated onto the CLs at room temperature (27 ± 1 ℃). The solution film thickness was set to 50 μm. Then, the sample was dried at room temperature and atmospheric pressure. The thicknesses of the CL and AEM are 47.5 ± 5.2 μm and 0.5 ± 0.2 μm, respectively, obtained from images (see Figure S4 and Table S1) taken via cross-sectional imaging with a focused ion beam scanning electron microscopy (Crossbeam 540 FIB-SEM, Zeiss). (see section 3.2)

Before electrochemical measurements, the samples are pre-conditioned in 1 M KOH (EMSURE®, Merck) for three hours. Then, the samples were washed thoroughly with DI water three times and kept wet yet not flooded before the GDE cell assembling.

3.2 Structural analysis

A Zeiss Crossbeam 540 focused ion beam scanning electron microscope (FIB-SEM) with a Gemini II column was used for thickness analysis. Before imaging, all samples were Gold sputter coated (108 Manual Sputter Coater, Cressington) to obtain a better conductivity.

Cross-sectional images of the GDEs were achieved by embedding the electrodes into epoxy resin (Epo Thin 2, Buehler). Afterward, the embedded samples were grinded (Silicon carbide grinding paper with grit 220 to 4000, Struers GmbH) and polished (MD-Mol polishing plate with 3 μm diamond polishing paste, ATM GmbH) using an automatic polishing machine (LaboForce-100, Struers GmbH). Finally, the embedded samples were imaged with a four-quadrant backscattering detector in compositional mode, which applies an accelerating voltage of 20 kV and 2 nA beam current.

Cross-sectional FIB-SEM imaging of cut-out samples was performed with 3 kV accelerating voltage and a current of 750 pA. A protective platinum layer was deposited via ion beam deposition using a gas injection system (Orsay Physics, MonoGIS). Then trenches were cut (30 kV accelerating voltage, 7 nA) and polished afterward with the focused ion beam (30 kV accelerating voltage, 700 pA and 100 pA).

3.3 Online dissolution measurements

The introduction of the acidic internal standard (IS) with constant concentration is usually for tracking and compensating the changes of the ICP-MS conditions during a measurement day. Moreover, for an alkaline analyte, the acidic IS also acts as a neutralizer to prevent the ICP-MS from being damaged by the alkaline condition. In this work, to achieve higher current density in our GDE half-cell, the concentration of the alkaline electrolyte, 0.1 M, is even double of the usually accepted maximum, 0.05 M. Hence, the flowrate of IS was increased around 3 times to 0.595 ± 0.005 mL·min^{-1}, to further dilute the alkaline analyte.

The collection efficiency (CE) is essential for quantifying the dissolution data and can be calculated using Equation S1, which has also been presented in our previous work [1].

$$CE = \frac{m_{Fe,ICP-MS}}{m_{Fe,total}} = \frac{m_{Fe,ICP-MS}}{m_{Fe,bulk,end} - m_{Fe,bulk,start} + m_{Fe,ICP-MS}} \quad \text{(S1)}$$

where $m_{Fe,total}$ is the total amount of Fe dissolved from the CL, $m_{Fe,ICP-MS}$ is the total amount of Fe collected into the ICP-MS, $m_{Fe,bulk,end}$ and $m_{Fe,bulk,end}$ are the amount of Fe in the bulk electrolyte after and before the measurement, respectively. The batch samples of bulk electrolytes were extracted right before, right after each measurement, and after the electrolyte was thoroughly mixed. The average of the latter two represents the bulk concentration after a measurement. The CE results are shown in Table S2.

.

Table S2. The parameters for basic normalization of the Fe dissolution data, including the loadings of the Fe-N-C GDE samples, the collection efficiencies and the flow rates of sample extraction during the electrochemical measurements.

Parameter	**Loading**	**Collection Efficiency**	**Flow Rate**
Unit	$mg \cdot cm^{-2}$	-	$ml \cdot min^{-1}$
Ar-1	1.40	0.19	0.1995
Ar-2	1.36	0.153	
O_2-1	1.34	0.190	0.20505
O_2-2	1.40	0.220	
O_2-M-1	1.30	0.170	
O_2-M-2	1.36	0.171	

Using Equation S2, basic normalization of the Fe dissolution raw data, [Fe] ($\mu g/L$), with CE, flow rate of the sample extraction, and the Fe-N-C loading, can be done. And the required data for the calculation are collected in

Table **S2.** S_{GDE} refers to the area of the GDE samples, 2.01 cm^2.

$$\frac{dFe}{dt}\left(\frac{pg_{Fe}}{s \times mg_{Fe-N-C}}\right) = \frac{[Fe] \times Flow\ Rate}{CE \times (Loading_{Fe-N-C} \times S_{GDE})} \quad \text{(S2)}$$

For the integration of dissolution peaks, the baseline of the dissolution peak is chosen as the straight line connecting the two endpoints of the integration interval. The first endpoint is the starting point of the galvanostatic/potentiostatic hold, and the second endpoint is where the Fe signal drops to background. Figure S7 demonstrates this integration method.

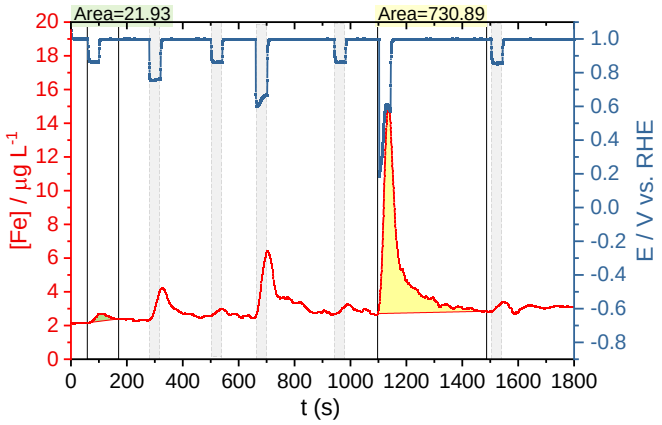

Figure S7. Demonstration of the integration method applied on the Fe dissolution data.

To further have a more concrete idea how much Fe species in the Fe-N-C catalysts was dissolved during the ASTs, the amounts of Fe dissolution $m_{Fe,\ dissolved}$ during ASTs were normalized to the total amount of Fe calculated from the loading (See Figure 3C). The calculation assumes that the commercial Fe-N-C catalyst comprises of 1 wt% of Fe, according to a previous work on this material.[2]

3.4 Electrochemical techniques

For comparing conditions in Ar and in O_2 environments, applying the same electrochemical protocol unfortunately would not result in the same or similar applied potential profiles. Because the potential determination of the working electrode (WE) requires post iR-compensation.[3] And in the condition with O_2, the uncompensated

resistances (R_u, 4 – 10.7 Ω in this study) vary with the applied current density, which in this work is between -5 and -125 $mA \cdot cm^{-2}$. This unpredictability of R_u leads to the difficulty in using potentiostatic holds for the conditions with O_2. Therefore, the two sets of measurements with O_2 were using galvanostatic techniques, and then the set with Ar was programmed with potentiostatic techniques accordingly.

4. Author contributions

Yu-Ping Ku: GDE-ICP-MS experimental design, data curation, formal analysis, scientific discussion, writing of original draft

Konrad Ehelebe: GDE-ICP-MS experimental design, scientific discussion, editing

Markus Bierling: SEM imaging, scientific discussion

Florian D. Speck: scientific discussion

Dominik Seeberger: scientific discussion

Karl J.J. Mayrhofer: scientific discussion and editing

Simon Thiele: scientific discussion and editing

Serhiy Cherevko: project conceptualization and administration, validation, scientific discussion, editing

5. References

1 Ehelebe, K. et al. Platinum Dissolution in Realistic Fuel Cell Catalyst Layers. *Angew. Chem. Int. Ed.* **60**, 8882-8888 (2021).

2 Hossen, M. M., Artyushkova, K., Atanassov, P. & Serov, A. Synthesis and characterization of high performing Fe-N-C catalyst for oxygen reduction reaction (ORR) in Alkaline Exchange Membrane Fuel Cells. *J. Power Sources* **375**, 214-221 (2018).

3 Ehelebe, K. et al. Evaluating Electrocatalysts at Relevant Currents in a Half-Cell: The Impact of Pt Loading on Oxygen Reduction Reaction. *J. Electrochem. Soc.* **166**, F1259 (2019).